INL/EXT-16-39915
Revision 0

Light Water Reactor Sustainability Program

Data Analysis of Different Nondestructive Testing Techniques to Monitor Concrete Structure Degradation due to Alkali-Silica Reaction

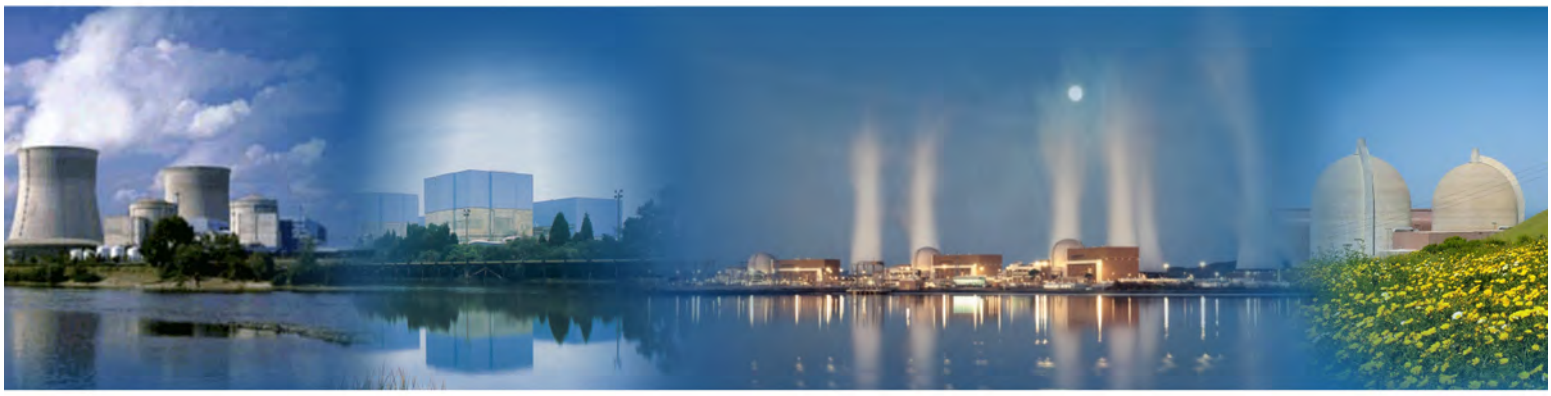

September 2016

U.S. Department of Energy
Office of Nuclear Energy

INL/EXT-16-39915
Revision 0

Light Water Reactor Sustainability Program

Data Analysis of Different Nondestructive Testing Techniques to Monitor Concrete Structure Degradation due to Alkali-Silica Reaction

Vivek Agarwal
Kyle Neal
Sankaran Mahadevan
Binh T. Pham
Douglas Adams

September 2016

Idaho National Laboratory
Idaho Falls, Idaho 83415

Vanderbilt University
Nashville, Tennessee 37235

Prepared for the
U.S. Department of Energy
Office of Nuclear Energy
Under DOE Idaho Operations Office
Contract DE-AC07-05ID14517

Light Water Reactor Sustainability Program

Data Analysis of Different Nondestructive Testing Techniques to Monitor Concrete Structure Degradation due to Alkali-Silica Reaction

INL/EXT-16-39915
Revision 0

September 2016

ABSTRACT

Assessment and management of aging concrete structures in nuclear power plants require a more systematic approach than simple reliance on existing code margins of safety. Health monitoring of concrete structures is performed in order to understand the current condition of a structure based on heterogeneous measurements and then produce high-confidence actionable information regarding structural integrity; this information can then be used to support operational and maintenance decisions. The proposed diagnosis and prognosis framework consists of four elements: health monitoring, data analytics, uncertainty quantification, and prognosis.

The objective of this ongoing research project is to evaluate several nondestructive examination (NDE) techniques for suitability in obtaining concrete-structure degradation data that can be used in the monitoring framework. This report focuses on degradation of concrete structures affected by the alkali-silica reaction (ASR). Controlled concrete bricks were cast and cured at various conditions to develop accelerated ASR degradation in a laboratory setting. Different NDE techniques (i.e., thermography, digital image correlation, mechanical deformation measurements, nonlinear impact resonance-acoustic spectroscopy, and vibro-acoustic modulation) were used to detect the damage caused by ASR. Heterogeneous data from multiple techniques were used for assessing damage of concrete samples that underwent different curing conditions. The NDE techniques were evaluated to determine if the data acquired were suitable for use in the online condition-monitoring framework for realistic concrete structures.

EXECUTIVE SUMMARY

One challenge facing the current fleet of light water reactors in the United States is age-related degradation of their passive assets, including concrete, cables, piping, and the reactor pressure vessel. As the current fleet of nuclear power plants (NPPs) continues to operate for 60 years or more, it is important to understand the current and the future condition of passive assets under different operating conditions that would support operational and maintenance decisions. To ensure safe and reliable long-term operation of the current fleet, the U.S. Department of Energy's Office of Nuclear Energy funds the Light Water Reactor Sustainability Program to develop the scientific basis for extending operation of commercial light water reactors beyond the current license extension period.

Among the different passive assets of interest in NPPs, concrete structures are investigated in this research project. Reinforced-concrete structures found in NPPs can be grouped into four categories: (1) primary containment, (2) containment internal structures, (3) secondary containments/reactor buildings, and (4) spent fuel pool and cooling towers. These concrete structures are affected by a variety of degradation mechanisms that are related to chemical, physical, and mechanical causes and to irradiation. Age-related degradation of concrete results in gradual microstructural changes (e.g., slow hydration, crystallization of amorphous constituents, and reactions between cement paste and aggregates). The purpose of structural health monitoring of concrete is to assess the current condition of a structure and to provide high-confidence actionable information regarding structural integrity and reliability. Vanderbilt University, in collaboration with Idaho National Laboratory and Oak Ridge National Laboratory, is developing a probabilistic framework for structural health monitoring and managing the condition of aging concrete structures in NPPs. This integrated framework includes four elements: (1) monitoring, (2) data analytics, (3) uncertainty quantification, and (4) prognosis.

The objective of this continuing research project is to obtain degradation data for concrete structures from a series of experiments conducted in controlled laboratory conditions. The ability of nondestructive examination methods to characterize concrete deterioration and correlate it with structural performance is also being assessed. This report focuses on concrete degradation caused by alkali-silica reaction (ASR). Concrete specimens were prepared to develop accelerated ASR degradation in a laboratory setting. Different nondestructive examination techniques (i.e., thermography, digital image correlation, mechanical deformation measurements, nonlinear impact resonance-acoustic spectroscopy, and vibro-acoustic modulation) were used to detect the damage caused by ASR. Heterogeneous data from multiple techniques were used for assessing the damage to concrete samples that underwent different curing conditions. The measured data can be linked to a probabilistic framework; the monitoring data were input to a Bayesian network for information fusion, uncertainty quantification of a diagnosis result, and prognosis in order to facilitate implementation of continuous online monitoring of realistic NPP structures.

Some of the outcomes of these experiments are as follows:

1. Three 9- × 5- × 2-in. concrete bricks were prepared and cured under various conditions to produce accelerated ASR degradation

2. The impacts of ASR development on specimen structures were examined using a number of interrogation techniques: thermography, nonlinear impact resonance-acoustic spectroscopy, and vibro-acoustic modulation
3. Experimental data from interrogation techniques found that these techniques can be used to generate data related to the assessment of degradation of concrete structures due to the impacts of ASR.

The experiments described in this milestone report are focused on concrete structural monitoring measurements and data analytics. This will support continuous assessment of concrete performance.

During the next phase of research, monitoring techniques will be refined for detection and localization of ASR in a reinforced-concrete specimen. The uncertainty quantification approaches and integration framework will be advanced further to handle large amounts of observation data. The resulting comprehensive approach will facilitate development of a quantitative, risk-informed framework that would be generalizable for a variety of concrete structures.

ACKNOWLEDGMENTS

This report was made possible through funding by the U.S. Department of Energy's Light Water Reactor Sustainability Program. We are grateful to Richard Reister of the U.S. Department of Energy and Bruce Hallbert and Kathryn McCarthy at Idaho National Laboratory for championing this effort. We also thank Jodi Vollmer and Jim H. Nelson at Idaho National Laboratory for technical editing and formatting of the report.

CONTENTS

FIGURES

TABLES

ACRONYMS

ASR	alkali-silica reaction
DIC	digital image correlation
NaOH	sodium hydroxide
NDE	nondestructive examination
NIRAS	nonlinear impact resonance-acoustic spectroscopy
NPP	nuclear power plant
SHM	structural health monitoring
VAM	vibro-acoustic modulation

Data Analysis of Different Nondestructive Testing Techniques to Monitor Concrete Structure Degradation due to Alkali-Silica Reaction

1. INTRODUCTION

Because many existing nuclear power plants (NPPs) continue to operate beyond their licensed life, their passive structures, systems, and components suffer deterioration that affects structural integrity and performance. Monitoring the condition of these elements of an NPP is essential for ensuring that its current and future conditions meet performance and safety requirements. This project focuses on concrete structures in NPPs. The concrete structures are grouped into the following four categories: (1) primary containment, (2) containment internal structures, (3) secondary containment/reactor buildings, and (4) other structures such as used fuel pools, dry storage casks, and cooling towers. These concrete structures are affected by a variety of chemical, physical, and mechanical degradation mechanisms, such as alkali-silica reaction (ASR), chloride penetration, sulfate attack, carbonation, freeze-thaw cycles, shrinkage, and mechanical loading (Naus 2007). The age-related deterioration of concrete results in continuing microstructural changes (e.g., slow hydration, crystallization of amorphous constituents, and reactions between cement paste and aggregates). Therefore, it is important that changes over long periods of time are measured and monitored, and that their impacts on the integrity of the components are analyzed to best support long-term operations and maintenance decisions.

Structural health monitoring (SHM) is required in order to produce actionable information regarding structural integrity that, when conveyed to the decision-maker, enables risk management with respect to structural integrity and performance. The methods and technologies employed include assessment of critical measurements, monitoring, and analysis of aging concrete structures under different operating conditions. In addition to the specific system being monitored, information may also be available for similar or nominally identical systems in an NPP fleet, as well as legacy systems. Therefore, Christensen (1990) suggested that assessment and management of aging concrete structures in NPPs requires a more systematic and dynamic approach than simple reliance on existing code margins of safety.

Through the Light Water Reactor Sustainability Program, several national laboratories and Vanderbilt University have begun research on concrete SHM in accordance with the proposed framework discussed in Mahadevan et al. (2014). The goal of this research is to enable plant operators to make risk-informed decisions on structural integrity, remaining useful life, and performance of concrete structures across the NPP fleet. The long-term research objective of this project is to produce actionable information regarding structural integrity to support operational and maintenance decision-making that is individualized for a given structure and its performance goals. In addition, the project supports the research objectives of three pathways under the Light Water Reactor Sustainability Program (i.e., the Advanced Information, Instrumentation, and Control Systems Technologies Pathway; the Materials Aging and Degradation Pathway; and the Risk-Informed Safety Margin Characterization Pathway).

Vanderbilt University, in collaboration with Idaho National Laboratory and Oak Ridge National Laboratory, is developing a framework for evaluating and forecasting the health of aging NPP concrete structures that are subject to physical, chemical, and mechanical degradation (Mahadevan et al. 2014; Agarwal and Mahadevan 2014). The framework will investigate concrete structure degradation by integrating the following four technical elements: (1) monitoring, (2) data analytics, (3) uncertainty quantification, and (4) prognosis. For details on each element of the proposed framework, refer to Mahadevan et al. (2014). The framework will enable plant operators to make risk-informed decisions on structural integrity, remaining useful life, and concrete structure performance. The demonstration performed at Vanderbilt University using various techniques to assess ASR degradation in controlled concrete specimens was reported in Mahadevan et al. (2016).

1.1 Objective and Layout of this Report

The objective of this report is to examine the use of vibro-acoustic techniques, nonlinear impact resonance-acoustic spectroscopy, and thermal infrared in assessing the effects of ASR on the integrity of concrete structures that are exposed to accelerated aging conditions in a laboratory. A series of experiments were conducted at the Vanderbilt University to provide sufficient degradation data in support of the framework (Mahadevan et al. 2014; Mahadevan et al. 2016) to examine and forecast the condition of aging concrete structures in NPPs. The remainder of the report is organized as follows:

- Section 2 discusses the technical basics of the ASR development and nondestructive examination (NDE) techniques to assess the effects of ASR on the integrity of concrete structures. The use of vibro-acoustic data for monitoring the development of ASR that occurred during accelerated aging of concrete structures is also discussed.
- Section 3 describes the preparation of specimens with ASR degradation and the laboratory experimental setup for the various NDE techniques.
- Data analysis of the collected monitoring data is presented in Section 4.
- A research summary and future activity are discussed in Section 5.

2. TECHNICAL BACKGROUND

2.1 Development and Impact of Alkali-Silica Reaction

The ASR is a reaction in concrete between the alkali hydroxides (K^+ and Na^+) in the pore solution and the reactive non-crystalline (amorphous) silica (S^{2+}) found in many common aggregates, given sufficient moisture. This reaction occurs over time and causes the expansion of the altered aggregate by the formation of a swelling gel of calcium silicate hydrate (C-S-H). Reactive silica is mainly provided by reactive aggregates and the alkalis by the cement clinker. ASR swelling results from the relative volume increase between the product and reactant phases involved in the chemical reaction. First, the products expand in pores and micro-cracks of the cementitious matrix. Once this free expansion space is filled, the swelling is restrained, and the product phases exert local a pressure on the surrounding concrete skeleton (Ulm 2000). Figure 1 depicts the mechanism of ASR (Kreitman 2011).

With water presence, the ASR gel increases in volume and exerts an expansive pressure inside the material, causing spalling micro- to macro-cracks (due to nonhomogeneous swelling related to non-uniform moisture distribution). As a result, ASR reduces the stiffness and tensile strength of concrete, because these properties are particularly sensitive to micro-cracking. ASR also can cause serious cracking in concrete, resulting in critical structural problems that can even force the demolition of a particular structure. The serviceability of concrete structures includes the resistance to excessive deflections, as well as a host of other durability concerns that can shorten the service life of a structure. Large surface crack widths and deep penetration of open surface cracks promote ingress moisture and any dissolved aggressive agents, such as chlorides. Additionally, the loss of concrete stiffness and potential for reinforcement yield are concerns for concrete deflection capabilities.

ASR is a complex chemical phenomenon, the rate and extent of which depend on a number of material and environmental parameters, and the interactions among parameters is not fully understood. This critical nature of ASR on premature concrete deterioration requires the quantitative assessment of ASR structural effects during service life (both in time and space). In particular, a combined experimental modeling investigation method is required to evaluate the impact of ASR on the dimensional stability of concrete structures. Although ASR has been identified as a cause of deterioration of numerous concrete structures and research has yielded some understanding of the mechanism of the reaction, the structural effects of ASR and how to best assess the extent of damage to existing structures remain major topics of ongoing research. This is because the expansion and cracking patterns (the most obvious sign of distress) caused by ASR affect both the concrete and the reinforcing

steel, but similar crack patterns can also be produced by other distress mechanisms (i.e., drying shrinkage and sulfate attack).

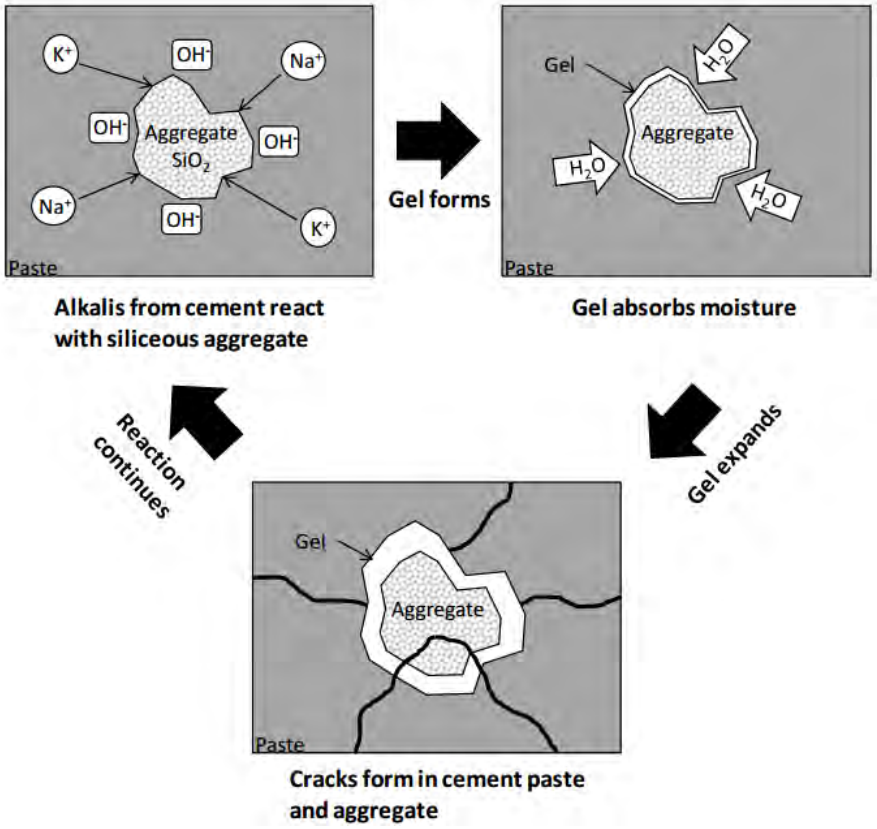

Figure 1. Mechanism of ASR (Kreitman 2011).

In the nuclear industry, a scoping study of ASR in concrete is performed to support future activities that include evaluating the effects of ASR on the structural capacity. From a safety perspective, the remaining capacity of a structure exhibiting distress due to ASR is an important factor in operational and maintenance management decisions. This is a challenging task for various reasons. First, the extent of the degradation will vary throughout the element as a function of the moisture content and as a function of the degree of restraint provided by the steel reinforcement. Also, it may be difficult to predict the properties of the concrete using certain testing results taken from the structure, because the size of the defects caused by the ASR may be large compared to a small structure, such as the cylinder (resulting in anomalously low tested strength), but small compared to the larger structure (suggesting there may be sufficient capacity). In addition, there is no reliable means of estimating the degree of the reaction in an existing concrete structure.

ASR can potentially affect concrete properties and performance characteristics, such as compressive strength, the modulus of elasticity, flexural stiffness, shear strength, and tensile strength. ASR can also impact material properties, but the structural performance of concrete elements depends on whether or not the concrete is unconfined or confined within reinforcing bars. The concrete core testing was conducted at the Seabrook nuclear power plant in February 2011 as part of the license renewal submission (NextEra Energy Seabrook 2012). These tests confirmed the presence of ASR-induced cracks in various structures within the plant and reduced modulus to some extent. The impact of reduced modulus on ASR-affected structures was evaluated. This evaluation found that the overall structure integrity was still within the strength requirements.

2.2 Diagnosis and Prognosis of Alkali-Silica Reaction Progress in Concrete

In NPPs, the concrete structures must have the strength required to resist dead weight, live loads, and seismic and other external events. For safety-related concrete structures that require extended periods of safe operations, a monitoring strategy is needed that can predict the future evolution of ASR to ensure that there is sufficient time to execute a safe cessation of operations. In this case, the evolution of mechanical properties as a function of the degree of ASR is required. For existing structures, an evaluation of the current state of the structure and an estimate of its future performance are critical. The diagnosis and prognosis in the structure monitoring procedure are based on an estimation of strength, modulus of rupture, and modulus of elasticity from the compressive strength of distressed concrete, which are critical parameters in a structural evaluation. Usually, the assumption is that these material properties decrease as a function of the degree of degradation, which is either the equivalent degree of free expansion or the extent of the chemical reaction.

The diagnosis and prognosis for the condition of a concrete structure leverage modeling of chemical, physical, and mechanical degradation mechanisms (such as alkali-aggregate reaction, chloride penetration, sulfate attack, carbonation, freeze-thaw cycles, shrinkage, and radiation damage) in order to inform monitoring and risk-management decisions. The alkali-aggregate reaction is currently receiving prominent attention among other applicable damage mechanisms for NPP concrete structures; these mechanisms are also included in the diagnosis and prognosis framework. The modeling and computational advances together with coupled-physics experiments and integrated multiple models through an appropriate simulation framework are leveraged to increase capacity and accuracy of monitoring technique. The combined model can be used for a prognosis of damage based on the current damage ascertained from the examination. The uncertainty quantification in the diagnosis can be propagated through the prognosis model to quantify uncertainty in the prognosis.

Details on the proposed health monitoring framework used for concrete structures are documented in Mahadevan et al. (2014). The framework will enable plant operators to make risk-informed decisions on structural integrity, remaining useful life, and performance of the concrete structure. The demonstration performed at Vanderbilt University using various techniques to assess ASR degradation in controlled concrete specimens was reported in Mahadevan et al. (2016). The success of this monitoring framework requires extensive experimental data in order to validate the modeling functional forms for predicting the condition of concrete structures exposed to specific operational conditions in an NPP. This validation process helps increase the prediction accuracy and reduce prediction uncertainty to a manageable level. By using the monitoring data taken from a number of different concrete designs that are representative of NPP concrete structures, a relationship will be developed between the degree of the ASR and the estimated mechanical properties. This correlation can be used to evaluate structural capacity in NPPs.

2.3 Nondestructive Evaluation Techniques for Monitoring Alkali-Silica Reaction

NDE techniques are essential for assessing ASR development in in-service concrete structures such as those in NPPs. For monitoring the ASR progression, the optical, thermal, acoustic, and radiation-based techniques are used for full-field imaging. Examples of these techniques include digital image correlation (DIC), infrared imaging, velocimetry, and ultrasonic and x-ray tomography. A particular consideration is the correlation between chemical degradation mechanisms and the observed degradation, which can be used to synergy between monitoring and prognosis. The standard test methods for determining the potential alkali-silica reactivity and for determination of the amount of time needed for concrete to change due to ASR are documented in ASTM C1567-13 and ASTM C1293-08b, respectively.

2.3.1 Infrared Thermography

Infrared thermography maps the thermal load path in a material. Cracking, spalling, and delamination in concrete would create a discontinuity in the thermal load path. Additionally, rebar and tensioning cables can be easily differentiating due to the difference in thermal conductivity coefficients between steel and concrete. Thermography has even been shown to detect debonding between the reinforcing steel and concrete. Infrared thermography can be either an active or passive monitoring technique. When heat is locally added to the structure to create a temperature gradient, the thermography is referred to as active. When only solar heat is used to provide heat to produce the temperature gradient, the thermography is considered passive. Passive infrared thermography is preferred, because it is less energy intensive. The Electric Power Research Institute showed the feasibility of infrared thermography by mapping a 450,000-ft^2 dam. During the 2 days that the Electric Power Research Institute spent mapping the dam, numerous potential delamination sites were identified (Renshaw et al. 2014). Kobayashi and Banthia (2011) combined induction heating with infrared thermography to detect corrosion in reinforced concrete. Induction heating uses electromagnetic induction to produce an increase in temperature in the rebar. When corrosion is present, it inhibits the diffusion of heat from the rebar to the surrounding concrete. Infrared thermography is then used to capture the temperature gradient. It was concluded that the temperature rise in corroded rebar is higher than in non-corroded rebar. A more-corroded rebar yields a smaller temperature rise on the surface, and the technique is more effective with larger bar diameters and smaller cover depths (Kobayashi and Banthia 2011). The current study is investigating the performance of infrared thermography as a means of identifying ASR.

2.3.2 Digital Image Correlation

Digital image correlation is an optical NDE technique that is capable of measuring the deformation, displacement, and strain of a structure (Bruck et al. 2012). During NPP routine pressure tests on containment vessels, when the internal pressure reaches 60 psi, it might be possible to use DIC to determine deformation of the concrete containment. DIC is capable of detecting surface defects, such as cracks, micro-cracks, and spalling, but is unable to detect any subsurface defects. The primary benefit of DIC is in measuring deformation; therefore, the ability of DIC to detect changes in the dimensions of the slab due to ASR gel expansion is of interest in this study. DIC requires a speckled pattern on the specimen to anchor observations at different points in time. This also presents a problem for the small brick specimens that are immersed in sodium hydroxide (NaOH) solution or water; the pattern is disturbed and partly dissolved in the NaOH solution. However, if the brick specimen is cured above water, DIC might be applicable.

2.3.3 Mechanical Deformation Measurement

The mechanical deformation measurement is a contact measurement technique. Calipers or an extensometer can be used to measure deformation along a linear distance. It is often convenient to glue on targets or cast nails into the concrete to provide more repeatable measurement points. In order to capture the ASR-induced concrete deformation, the measurement device needs to be accurate to within a few hundred microns. Most high-resolution mechanical measurement devices have a relatively short measuring span (i.e., 1 ft or less). This makes them ideal for laboratory experiments but limits their applicability in real-world structures without using a significant number of targets glued to the structure.

2.3.4 Nonlinear Impact Resonance-Acoustic Spectroscopy

All solids have natural periods of vibration, also known as resonant frequencies, at which solids tend to vibrate when excited. This is a function of the dimensions, stiffness, density, and boundary conditions (external restraint) of the solid. If two objects that have different stiffness, but are otherwise identical, are compared, the stiffer object will have a higher resonant frequency (shorter natural period). ASR and delayed ettringite formation reduce concrete's stiffness, which can be detected by measuring the resonant frequency. Linear test methods have proven reasonably effective for locating larger defects, but test

methods based on nonlinear behavior may be many times more sensitive to micro-cracks and distributed damage characteristics of ASR.

Nonlinear impact resonance-acoustic spectroscopy (NIRAS) is an NDE technique that uses the vibrational response of a structure to classify damage. NIRAS was developed at Georgia Tech to detect ASR-induced damage in concrete (Lesnicki et al. 2014). NIRAS operates based on the following idea: a linear system has the same natural frequency regardless of the amplitude of the excitation force. In contrast, for nonlinear systems, the resonant frequency experiences a downward shift as the force of the impacts increases, and this shift is increasingly prominent in specimens with micro-cracking. Figure 2 shows the resonant frequency shift for a nonlinear system as the amplitude of the excitation force increases (Mahadevan et al. 2016).

The nonlinearity parameter is commonly used to quantify the severity of damage. The nonlinearity parameter is calculated as a scaled slope of the input force amplitude versus the frequency shift. It is well known that concrete samples with more severe damage generally have a larger value for the nonlinearity parameter (steeper slope). On the other hand, a sample in pristine condition (or linear structure) should have no frequency shift with increasing input force amplitude, and then its nonlinearity parameter would be 0. Figure 3 shows an example of the frequency shift plot as a function of the input force amplitude for a brick specimen. The frequency shifts corresponding to the input force amplitudes are taken from NIRAS results presented in Figure 2. The nonlinearity parameter was calculated as a slope of the fitted line (black line) to measured data points (cross symbols); this parameter equals 0.1219 (Figure 3). This positive (or non-zero) slope indicates that the specimen structure is nonlinear or damaged to some extent.

Because ASR causes micro-cracking within the concrete, which creates nonlinearity, it is believed that NIRAS can be used to detect damage in concrete before the cracking is visible on the surface. Because NIRAS is a global vibrational response technique (i.e., it measures shifts in resonant frequency), it is better suited for small laboratory concrete specimens than large concrete structures. For example, if a large concrete structure had a small patch of ASR growth, it is unlikely that NIRAS would be able to detect the growth, because it will have a minimal effect on the natural frequency of the structure.

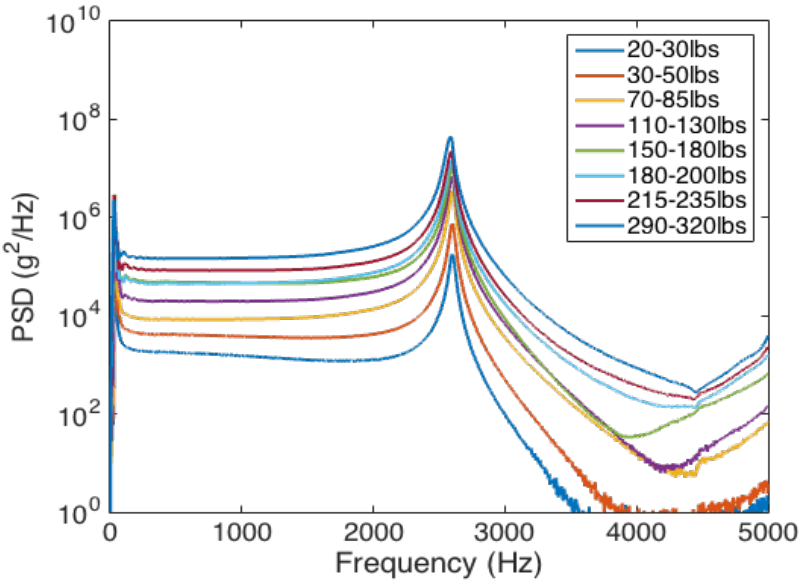

Figure 2. Results from a concrete brick, showing frequency shift with increasing input force amplitude.

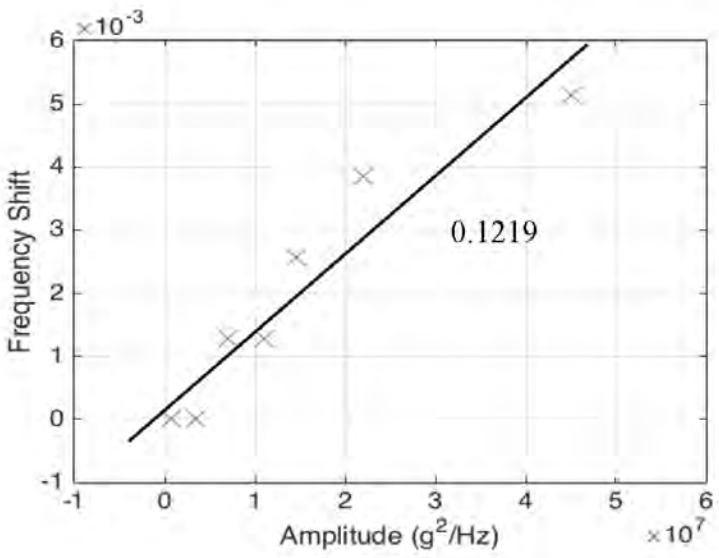

Figure 3. Calculation of nonlinearity parameter for the brick specimen.

2.3.5 Vibro-Acoustic Modulation

Vibro-acoustic modulation (VAM) is a nonlinear vibration technique in which the structure of interest is excited using a combination of specific frequencies and the response is recorded. VAM is also known by other names, such as nonlinear wave modulation spectroscopy. The VAM technique assumes that an undamaged structure can be represented by a linear system while the representation of a damaged structure must include nonlinearity, which is the result of the generation of sideband responses. VAM is a nondestructive testing technique that has been successful in detecting nonlinearities in various materials, including detecting ASR-induced damage in concrete (Chen 2008; Chen 2009).

VAM works by exciting a structure with two frequencies of vibration simultaneously. The low-frequency input is termed the "pump," and the high-frequency input is termed the "probe" (Kim et al. 2014). Interaction of the pumping and probing signals can help identify the presence of nonlinearities in the system. As the pumping signal causes the crack to open and close (shown in Figure 4), the effective cross-sectional area that the probing signal can travel through also changes. Thus, the amplitude of the probing signal transmitted through the beam changes with the phase of the pumping signal. In the equations below, the time domain representation for three scenarios is given. *Equation (1)* shows the response of a system to just the pumping signal, *Equation (2)* shows the response of a linear system to a pumping and probing signal (i.e., principle of superposition is maintained), and *Equation (3)* shows the response of a nonlinear system to pumping and probing signals. The third term in *Equation (3)* represents the modulation, which manifests itself in the frequency domain as a convolution of spectra.

$$\cos(\omega_1 t) \tag{1}$$

$$\cos(\omega_1 t) + \cos(\omega_2 t) \tag{2}$$

$$\cos(\omega_1 t) + \cos(\omega_2 t) + \cos(\omega_1 t) * \cos(\omega_2 t) \tag{3}$$

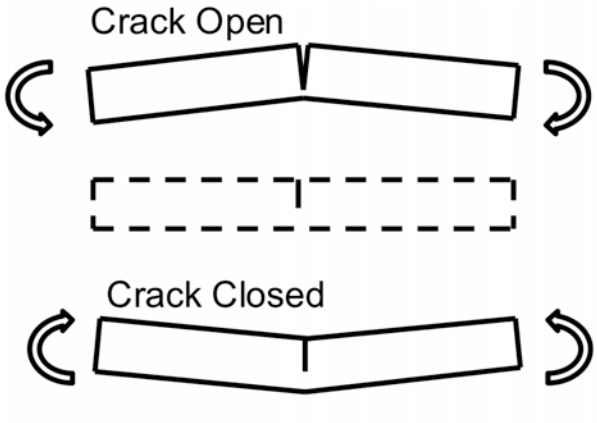

Figure 4. VAM representation of system response to pumping signal.

The modulation described in *Equation (3)* will produce sidebands (product of two distinct frequency signals) around the probing frequency, which is illustrated in Figure 5, when no noise signal is present. Similar to NIRAS, the resonant frequency is determined in this technique as well. However, in VAM, the data are inspected for modulation about the probing frequency. This modulation indicates the nonlinearity within the system. Realistic VAM results for the three brick samples (i.e., A, B, and C) are shown in Figure 6 (Mahadevan et al. 2016). Several potential damage indices based on the response spectrum properties were considered, as follows:

- Ratio of sideband amplitude to probe or pump amplitude
- Ratio of sideband bandwidth power to probe or pumping power (integral under power spectral density)
- Percent of total power present in sideband power.

It is worth noting that the fundamental understanding of the physics behind the nonlinear vibration phenomenon in solids is not well understood. Also, various nonlinear mechanisms exist in solids and typically are characterized as either elastic or dissipative. Compounding contributions from each of the different mechanisms may be difficult to separate. For example, compounding nonlinear effects from surface-to-surface bonding and other tangible interfaces could mask sidebands indicative of ASR-induced damage. Sideband amplitude response has been known to be heavily dependent on the system excitation and boundary conditions. In addition, sideband amplitude was observed decreasing as fatigue cracks grew well past initiation. This observation could potentially be explained by the increasing dominance of global stiffness reductions as cracks grow to large lengths as compared to the significance of breathing cracks at smaller crack lengths.

In general, the influence of structural configuration, excitation voltage, boundary conditions, and crack geometry should be thoroughly addressed before fielding SHM applications using nonlinear acoustics. Thus, the VAM technique is more suitable for damage detection than for assessing the extent of the damage (Vehorn 2013).

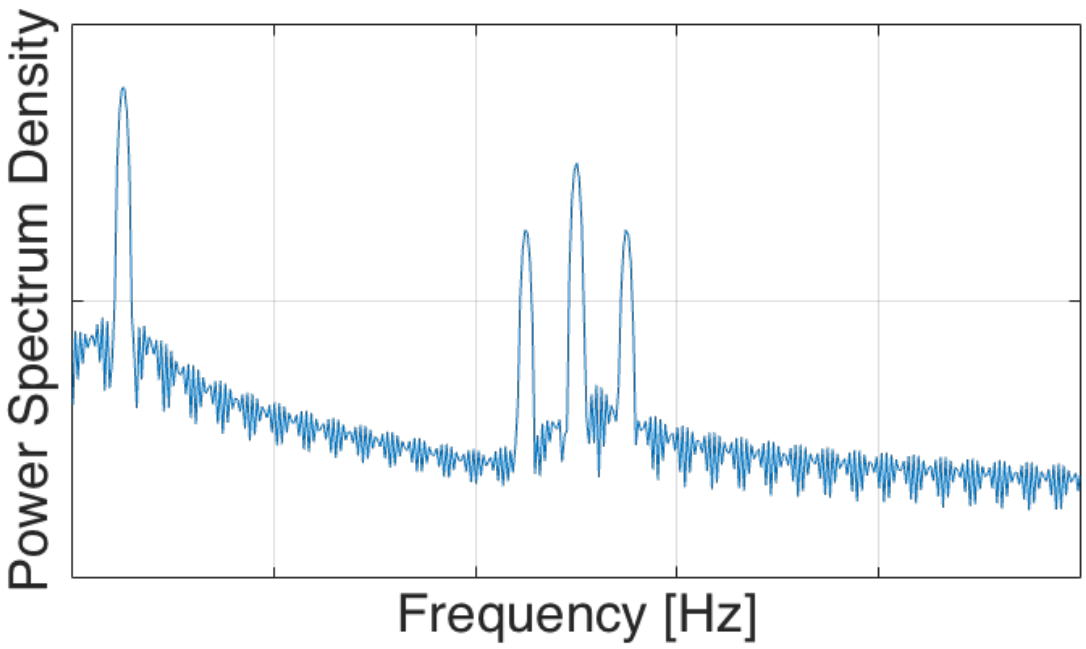

Figure 5. Sidebands generated in the presence of damage, indicating the structure nonlinearity.

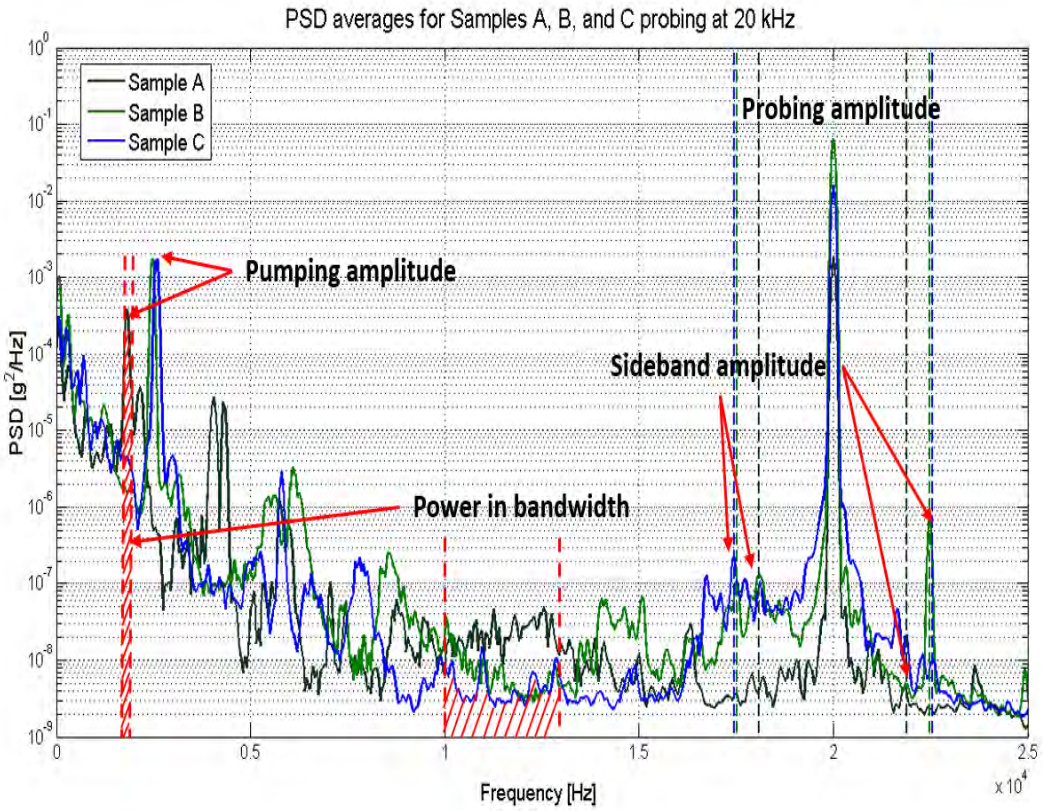

Figure 6. VAM results: power spectrum density in the frequency domain for three sample bricks (Mahadevan et al. 2016).

3. EXPERIMENTAL SETTING

This research investigates the monitoring of degradation in concrete due to ASR via VAM full-field imaging techniques. Effective combinations of full-field techniques need to be identified for different types of concrete structures under different loading and operating conditions. The monitoring techniques are studied with concrete samples constructed and cured in the laboratory. The concrete samples are described in the next subsection.

3.1 Sample Preparation and Curing

The ASR is a slow-developing process that can take several decades to become visible and result in failure. In the laboratory, aggressive conditions are applied to accelerate this process so the degradation progression and corresponding data can be observable. In this study, the NaOH in the mix water or placing the cured concrete in a NaOH solution is used to create a concrete pore solution with increased pH capable of inducing ASR. At the same time, highly reactive siliceous aggregates or glass are used to provide an enriched source of silica. In addition, the relative humidity in concrete is essential for ASR, affecting both kinetics and magnitude. Water plays the role of the solvent for the silica dissolution and intervenes as transport media for the diffusion of ions through the pore solution. Water is also a necessary compound for the formation of the various reaction products (gels, precipitates, crystals, etc.). Finally, the concrete specimens are cured at higher temperatures (i.e., 60 to 80°C) to accelerate ASR, because ASR mechanisms are thermo-activated. The high concentration of alkali hydroxides and silica at high temperature promotes the occurrence of ASRs. The high curing temperature (>70°C) also promotes the formation of the internal sulfate attack (Giannini et al. 2012). Therefore, using these three accelerating features, the ASR gel can be produced in the laboratory environment, leading to cracks in concrete within several months.

3.1.1 Concrete Bricks

Three 9- × 5- × 2-in. concrete bricks, designated U1, U2, and U3, were cast, and the development of ASR was monitored over time using several NDE techniques. Powdered silica was used for aggregate in the three concrete bricks in the ratio of four parts cement to one part silica by weight. Brick U1 was not subjected to NaOH, which causes increased alkalinity and promotes ASR, and thus represents a baseline specimen. Bricks U2 and U3 were exposed to NaOH but by different means. Brick U2 was submerged in a 1N NaOH bath, per ASTM C1567-13 specifications, during accelerated curing. Brick U3 was cast using a NaOH solution for the mix water to increase the alkali content to 1.25% by mass of cement according to ASTM C1293-08b and was cured suspended over a tub of water to create 100% relative humidity. One goal of this study was to see which method of applying NaOH was more effective in promoting the development of ASR. A summary of the composition and curing conditions for Bricks U1, U2, and U3 is presented in Table 1.

Table 1. Summary of composition and curing conditions for Bricks U1, U2, and U3.

Brick	Aggregate	Sodium Hydroxide	Accelerated Curing
U1	Powdered silica	None	None (baseline)
U2	Powdered silica	In curing bath	60°C, submerged in NaOH solution
U3	Powdered silica	Mix water	60°C, 100% relative humidity

3.1.2 Vibration-Based Nondestructive Examination Setup

In addition to length measurements, the three concrete bricks were tested over time using two vibration-based NDE techniques: (1) NIRAS and (2) VAM. Both techniques detect nonlinearities within a concrete structure. In the concrete bricks, nonlinearity of the spectroscopy images could occur due to micro-cracking, cracking, or even the presence of ASR gel. NIRAS of a nonlinear structure is observable because of the shifts in the natural frequency (Chen et al. 2010; Lesnicki et al. 2012). A linear structure

will have a constant resonant frequency regardless of the amplitude of the excitation, but a highly nonlinear structure will display a decreasing resonant frequency with increased excitation amplitude. The nonlinear parameter can be calculated as the slope of resonant frequency shift versus amplitude of the impact force.

Figure 7 shows the VAM test setup. The concrete brick was placed in a simply supported condition for this test. The modal hammer struck the bricks to create an impulsive load that was used as the low-frequency "pump." A piezo-stack actuator acted as the high-frequency "probe." A tri-axial accelerometer measured the sample's response. A sampling frequency of 51.2 kHz facilitated the high-frequency probe, and a sampling period of 0.1 second resolved modulated sidebands. Variance impact forces and probing frequency were recorded for evaluation. Optimal pumping and probing frequencies are system dependent; however, in general, a higher probing-to-pumping ratio is preferred.

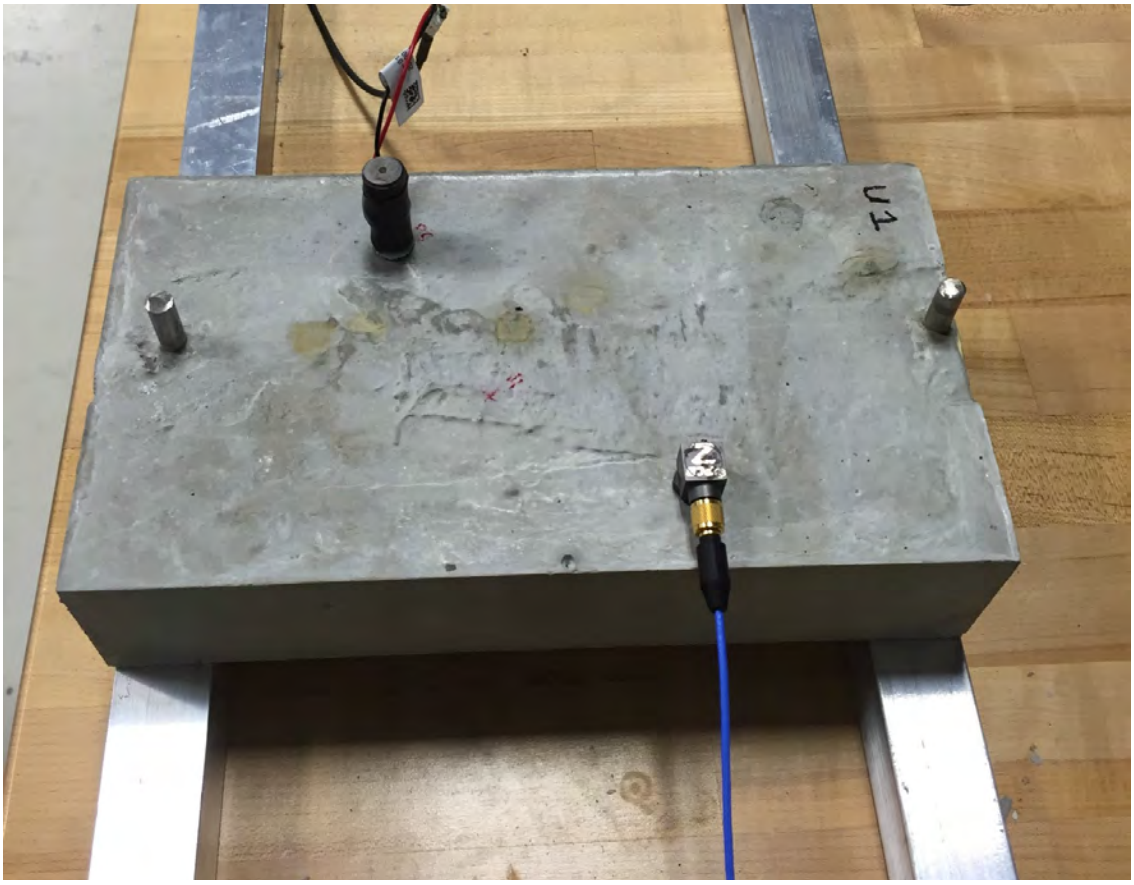

Figure 7. VAM test setup for ASR detection in brick samples.

4. ALKALI-SILICA REACTION DETECTION RESULTS

4.1 Mechanical Deformation Measurement

The characteristic signature of ASR in damaging a concrete structure is expansion. Steel pegs were cast in the concrete bricks to provide points for repeatable measurements to be taken while the concrete was curing, as shown in Figure 8. Measurements of the bricks' lengths were taken multiple times as the bricks were curing. Table 2 tracks the length between the two steel pegs on each of the concrete bricks as a function of curing time. The baseline brick, U1, decreased in length, especially during the first month, and length measurements of the ASR-aggressive curing bricks (U2 and U3) show slight expansion. The

reduction in length of the baseline U1 is associated with normal shrinkage of concrete over time, whereas the increase in length of accelerated ASR bricks, U2 and U3, indicates expansion of concrete due to the forming of ASR gel.

Figure 8. U bricks during curing with wood holding steel pegs in place.

Table 2. Length of U bricks across time measured between steel pegs.

	Length (inches)					
Brick	**11-Feb**	**1-Mar**	**17-Mar**	**7-Apr**	**7-Jun**	**11-Jul**
U1	8.265	8.250	8.245	8.243	8.242	8.241
U2	8.180	8.185	8.184	8.184	8.185	8.186
U3	8.195	8.197	8.198	8.199	8.200	8.200

Figure 9 depicts the length change ratio of the three bricks as a function of curing time. The change ratio in percent is calculated as follows:

$$\Delta l = 100\,\frac{l_i - l_0}{l_0} \tag{4}$$

where l_0 and l_i are the lengths between the steel pages measured during the first day of the test (February 11, 2016) and on Day *i*, respectively. These plots show that length change ratios for the accelerated ASR bricks, U2 and U3, are similar (red and green lines, respectively, in Figure 9), and they have a much smaller length change ratio than Brick U1 (blue line in Figure 9).

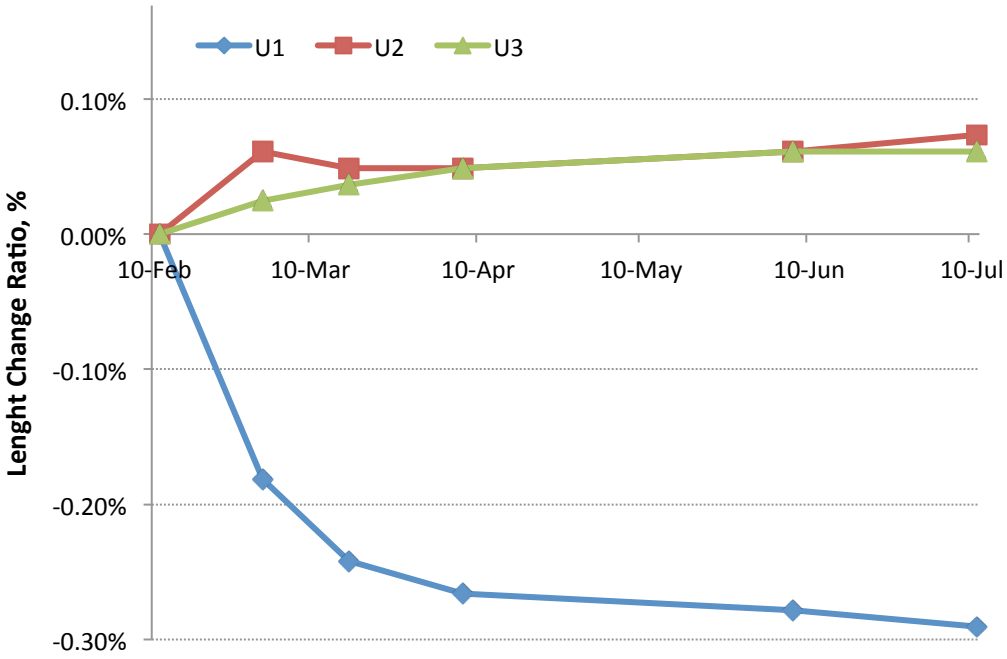

Figure 9. Change in length of bricks as function of time.

4.2 Nonlinear Impact Resonance-Acoustic Spectroscopy

Raw acceleration data are converted from the time domain to the frequency domain using the fast Fourier transform in MATLAB. In the frequency domain, the first resonant frequency is identified. The shift in resonance frequency of a concrete sample occurred when an increase in input force amplitudes indicated the concrete system was nonlinear (i.e., there was micro-cracking due to ASR). The severity of concrete damage was characterized by nonlinearity in the parameter, which was calculated by simply finding the scaled slope between the input force amplitude versus the frequency shift. It is well known that concrete samples with more severe damage generally have a larger nonlinearity parameter (or steeper slope). If a sample is in pristine condition, it should have no frequency shift with increasing input force amplitude; then the nonlinearity parameter equals 0.

4.2.1 Baseline Brick U1 Results

Brick U1 served as a baseline sample, which was not exposed to NaOH. However, Figure 10 shows hairline cracks visible on the surface of baseline Brick U1 after 5 months of curing, which results in an increasing shift in resonance frequency with increasing input force amplitude, as shown in Figure 11. Even though the ASR is unlikely (or insignificantly) to occur in Brick U1, the observed cracks are due to other damage mechanisms in concrete. This example demonstrates that vibration-based examination techniques have difficulty in distinguishing the cause of concrete damage; either it is from ASR or from other damage mechanisms in concrete.

Figure 10. Hairline cracks are visible on the surface of Brick U1.

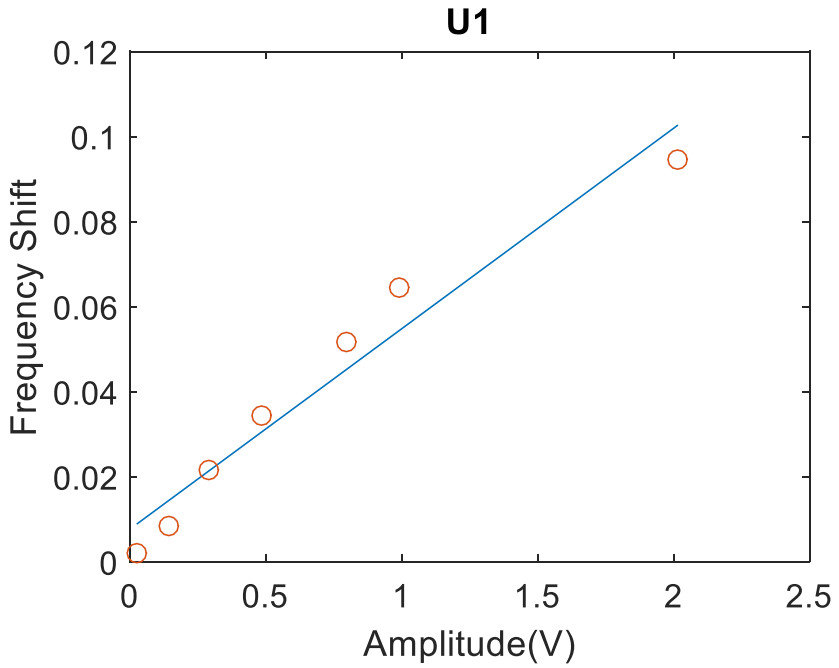

Figure 11. Frequency shift as a function of input force amplitude for the baseline Brick U1.

4.2.2 ASR-Accelerated Brick U3 Results

Brick U3 was exposed to water with NaOH solution to increase the alkali content to 1.25% by mass of cement and was cured over a tub of water to provide 100% relative humidity. Figure 12 shows the responses of Brick U3 in the frequency domain for various input force amplitudes ranging between 20 and 320 lb, which were taken on the first day of testing. The resonant frequency (at the peak of response) remained at the same level of 2,480 Hz as the impact force amplitude increased, which indicated that the concrete structure was linear, as expected. After 5 months of aggressive curing, Brick U3 exhibited a slight resonant frequency shift as the impact force amplitude increased, as shown in Figure 13 (the peaks moved to the left when input force increased). Additionally, the resonant frequency at the lowest input force then increased to 2,800 Hz, which represents a large shift from resonance frequency at the beginning of the test (an increase of 320 Hz). This increase in resonant frequency might have been caused by the increase in stiffness of the concrete as it cured.

From the results, it is clear that damage was detected in Brick U3 after 5 months of ASR accelerated curing. At that point, Brick U3 had expanded in length (green line in Figure 9), which indicates the formation of ASR gel leading to concrete expansion instead of concrete shrinkage during normal curing as in Brick U1 (blue line in Figure 9).

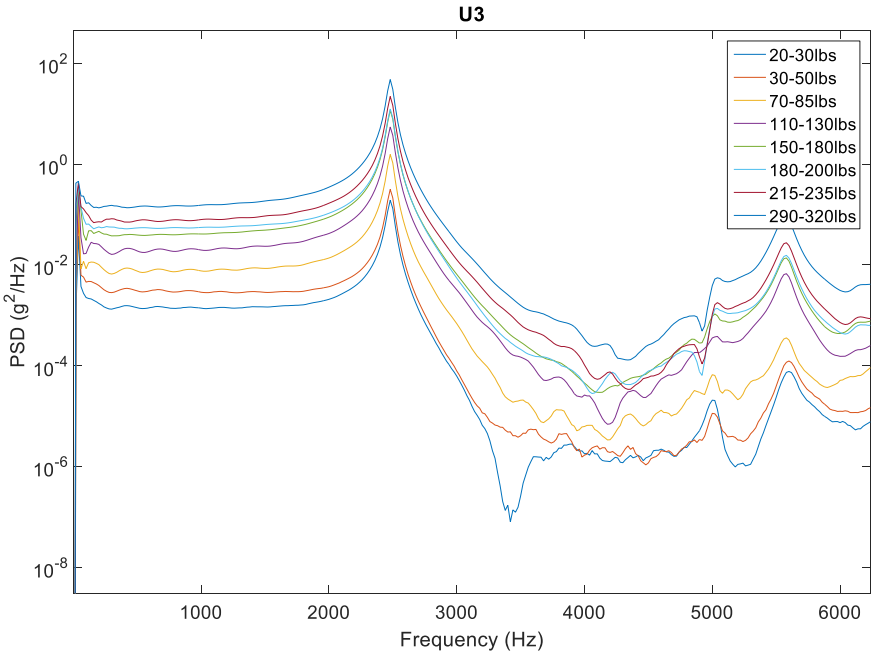

Figure 12. No resonant frequency shift observed on February 11 (Day 1 of the test) for Brick U3.

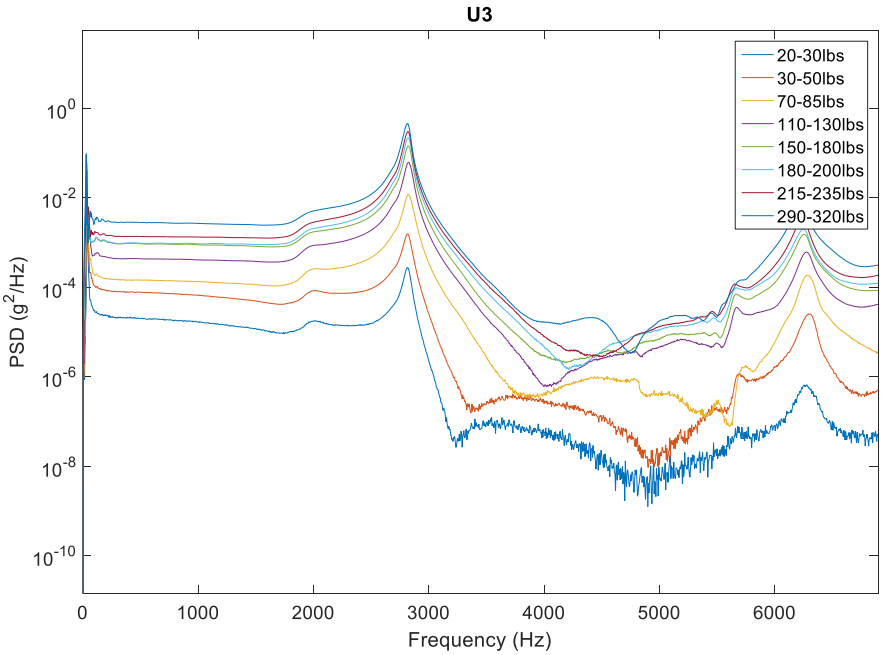

Figure 13. Resonant frequency shift observed on February 11 (5 months later) for Brick U3.

4.2.3 Nonlinearity Parameter for Bricks U1, U2, and U3

For this report, the damage index was calculated as the ratio between the sideband amplitude and the pump amplitude, as shown similarly to plots in Figure 6.

Table 3 and Figure 14 present nonlinearity parameters of the three bricks calculated at different measurement dates. Initially, all three bricks (U1, U2, and U3) had linear structure, as indicated by 0 nonlinearity parameters. As the cure progressed, their nonlinearity parameters increased over time, indicating that the structures became nonlinear. The following observations can be made:

- For Brick U1: The nonlinearity parameter increased soon after 1 month of curing and had the highest value over time among the three bricks (blue line in Figure 14). This is explained by the formation of multiple hairline cracks as it cured (Figure 10). The dry curing condition for Brick U1 led to quick concrete shrinkage and form hairline cracks.
- For Bricks U2 and U3: Because of the presence of moisture in wet (U2) or humid (U3) curing conditions, the concrete structures expanded over time instead of shrinking, as was the case for Brick U1 due to accelerated formation of ASR. However, during the first 2 months of curing, the formation of hairline cracks was unlikely, and the ASR gel was negligible, so the concrete structures of these two bricks remained linear, as indicated by 0 linearity parameters.
- For Brick U2: After submerging it in the 1N NaOH bath, Brick U2 expanded the most during the first month of curing, and it then maintained more or less the same length after that first month, as shown by the red line in Figure 9. The nonlinearity of Brick U2 increased during the third month and then decreased during the last 2 months. One possible explanation of this behavior could be that, at first, an abundance of water led to a higher expansion rate of the forming ASR gel, and later, the shrinkage inherent in concrete curing reduced the expansion of the ASR gel.

- For Brick U3: Curing in a 100% humid condition, Brick U3 expanded gradually over time, which can explain the increase of its nonlinearity parameter after months of curing. Brick U2 had the least nonlinearity coefficient among the three tested bricks, which could indicate the least damage due to ASR gel.
- In summary, NIRAS data show that curing concrete in a dry condition leads to more damage (or nonlinear structure) due to cracks in concrete as it cures, and that the presence of moisture during curing can prevent this effect, even though it increased development of ASR.

Table 3. Nonlinearity parameter of U1, U2, and U3 over time.

Brick	Curing Condition	NIRAS Nonlinearity Parameter					
		11-Feb	1-Mar	17-Mar	7-Apr	7-Jun	11-Jul
U1	Baseline	0	0.0026	0.0325	0.0257	0.0472	0.0937
U2	Submerged in 1N NaOH bath	0	0	0	0.014	0.0104	0.0043
U3	1.25% of NaOH and 100% humidity	0	0	0.0009	0.0034	0.0027	0.0044

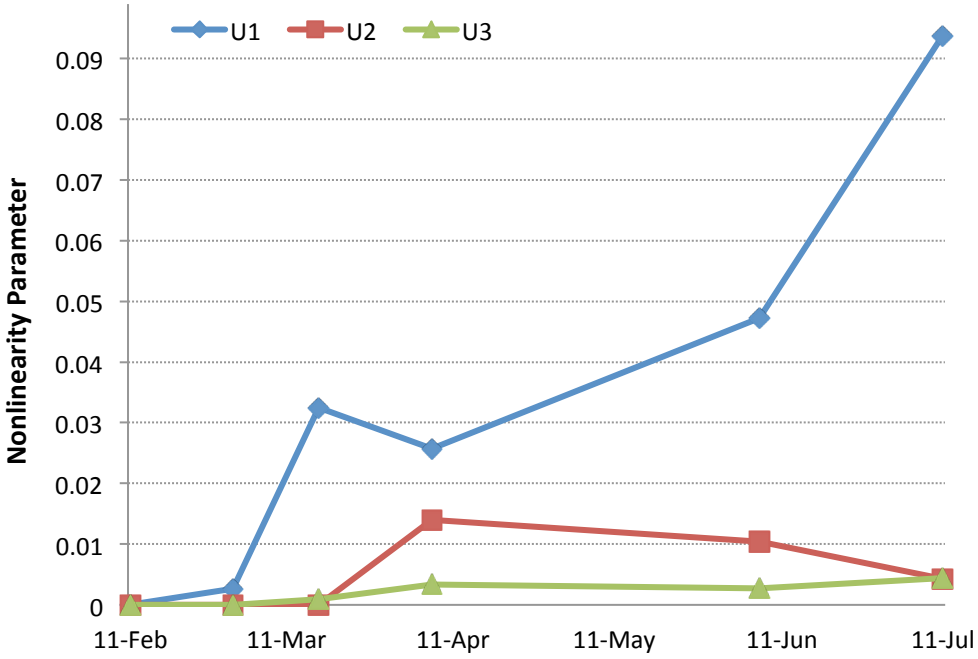

Figure 14. Nonlinearity parameters of Bricks U1, U2, and U3 as function of time.

4.3 Vibro-Acoustic Modulation

During the VAM test, the modal hammer struck the bricks to create an impulsive load that was used as the low-frequency pump, and the piezo-stack actuator acted as the high-frequency probe. Then, the triaxial accelerometer measured the sample's response. A sampling frequency of 51.2 kHz facilitated the high-frequency probe, and a sampling period of 0.1 second resolved modulated sidebands. A probing frequency of 14 kHz was used, and the response from eight hammer impacts was averaged together.

Figure 15 depicts the power spectral density of Brick U3 taken after 5 months of accelerated curing. From the VAM results, as shown in Figure 15, a damage index was calculated as the ratio of the sideband amplitude to the pump amplitude. The VAM damage indices of the three tested bricks at each measurement date are given in Table 4 and Figure 16. The data show increasing damage indices for each of the bricks over time.

For comparison, both NIRAS (Figure 13) and VAM (Figure 16) results identified the increased damage over time that was caused by the ASR gel expansion, as seen in Bricks U2 and U3 (blue and green lines, respectively). On the other hand, the damage in Brick U1 is likely due to concrete shrinkage. The amount of damage and deformation is fairly similar for Bricks U2 and U3, which indicates that the NaOH water bath curing and the 100% humidity curing with a higher concentration of NaOH produced comparable results. Also, strong correlation between the VAM damage index and the NIRAS nonlinearity parameter increases the confidence in potential use of VAM for ASR detection in concrete.

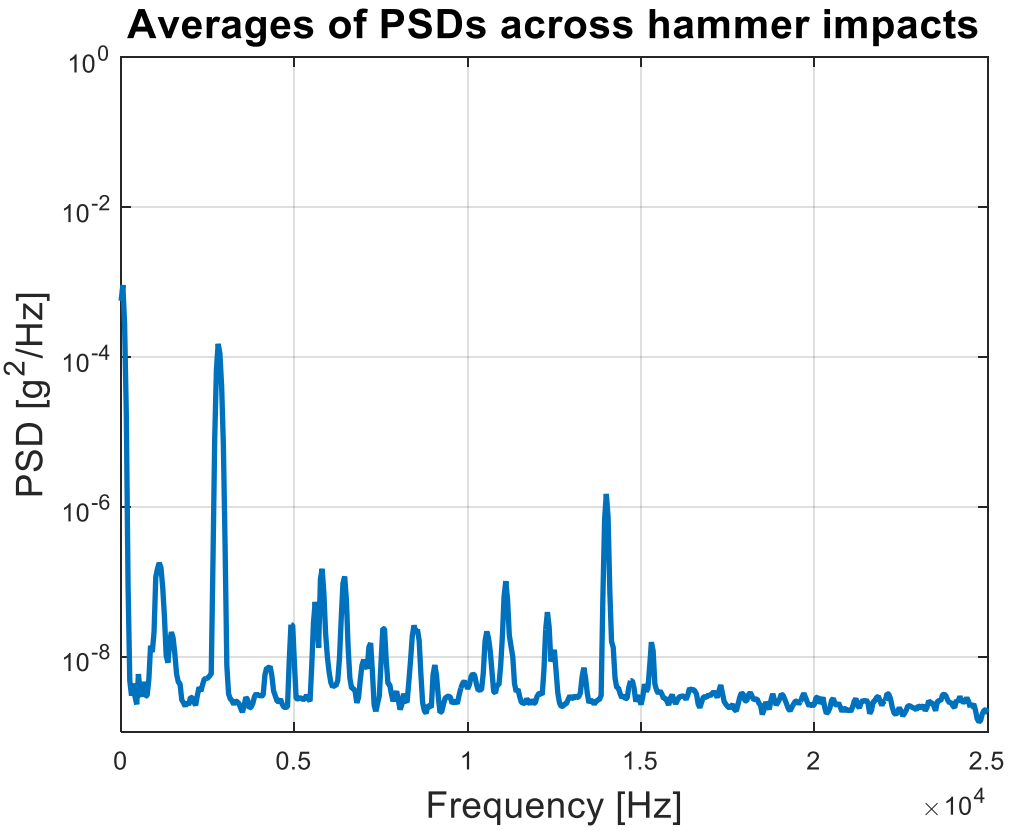

Figure 15. VAM results for Brick U3 after 5 months of curing.

Table 4. Damage indices from VAM for all three bricks over time.

	VAM Damage Index					
Brick	**11-Feb**	**1-Mar**	**17-Mar**	**7-Apr**	**7-Jun**	**11-Jul**
U1	1.96E-02	5.28E-03	4.67E-02	2.18E-01	1.71E+01	1.93E+01
U2	7.51E-03	4.76E-01	2.47E-01	4.84E-03	1.67E+00	9.48E+00
U3	2.77E-04	3.73E-03	3.76E-03	1.82E-04	8.36E-04	1.75E+00

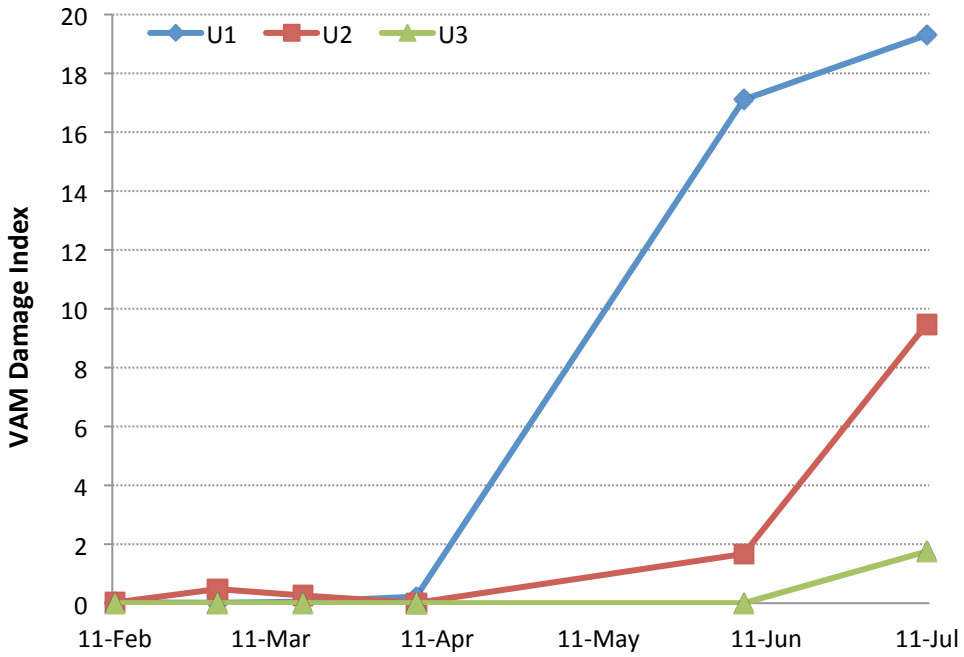

Figure 16. VAM damage indices for Bricks U1, U2, and U3 as function of time.

4.4 Infrared Thermography

The infrared thermography study of Bricks U1, U2, and U3 is reported here (see Table 1 for a summary of the composition and curing conditions for these bricks).

The hypothesis is that formation of ASR should change the heat conductivity within the brick. Therefore, there would be a temperature difference between the dry-cured and NaOH-water-cured bricks at each time stamp. The temperature difference between the dry-cured data and NaOH-water-cured data at each time stamp is selected to be the baseline temperature difference. The corresponding temperature differences for Bricks U2 and U3 are expected to be different from the baseline brick, U1. Based on the baseline brick, upper bound and lower bound values (at each point in time) were selected for the temperature difference between dry-cured data and NaOH-water-cured data. If the temperature difference was outside the bounds, then a change in heat conductivity was indicated, implying the formation of ASR. To set boundaries, maximum and minimum values of the temperature difference were selected among all pixels between the dry-cured data and NaOH-water-cured data at each time stamp.

The temperature measurements from an infrared camera were verified by readings from multiple thermocouples. Five thermocouples were installed on concrete samples at different locations (as shown in Figure 7 for Brick B2), and the temperature data were collected along with data from infrared imaging measurements for verification purpose. Post processing of infrared images did not impact the verification process. Figures 18–22 show temporal temperature profiles, which are measured by thermocouple (circle symbols) and infrared-camera (solid line) at five thermocouple locations for comparison. The decent match between thermocouple and infrared-camera temperature measurements at all five locations indicates that infrared camera can be used to nondestructively measure temperature of a concrete structure, when installation of thermocouples is not possible or desirable.

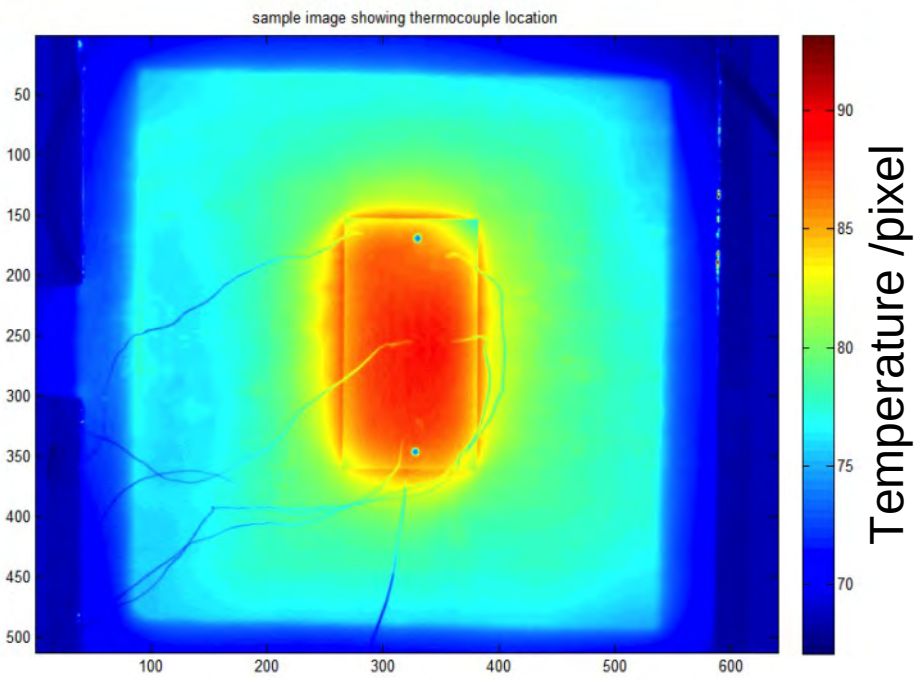

Figure 17. Thermal image of Brick U2 showing five thermocouple locations.

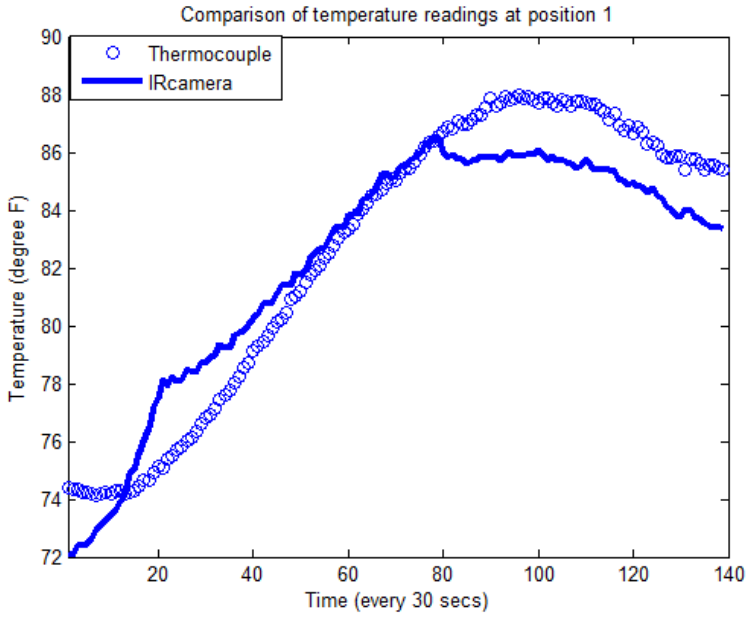

Figure 18. Comparison of infrared-camera and thermocouple measurement s over a 30-second interval at Position 1.

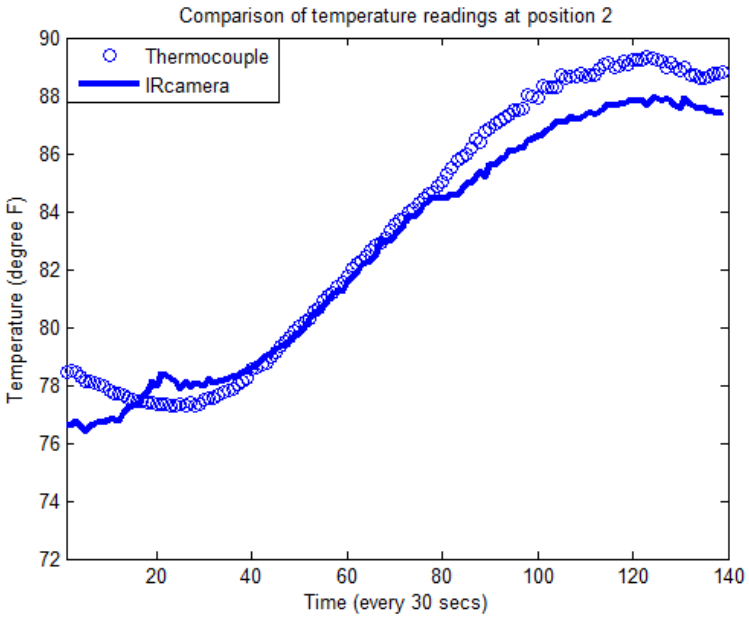

Figure 19. Comparison between infrared-camera and thermocouple measurements over a 30-second interval at Position 2.

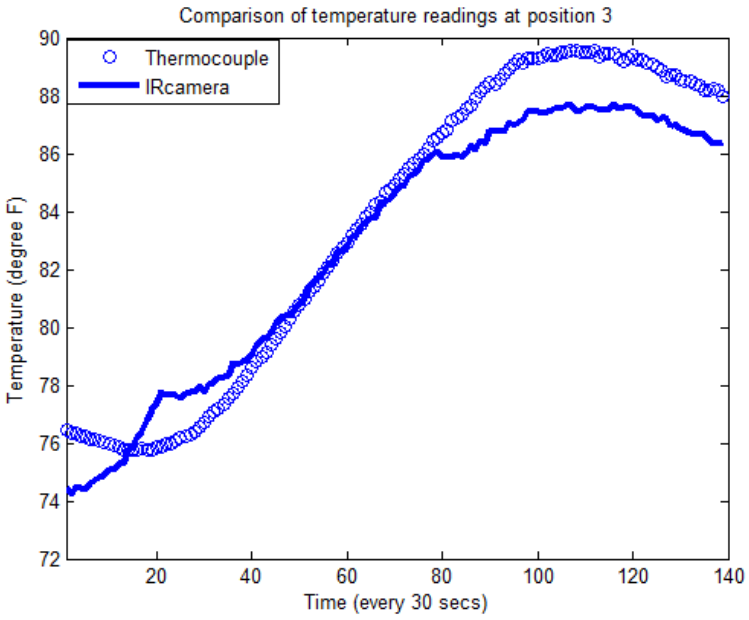

Figure 20. Comparison of infrared-camera and thermocouple measurements over a 30-second interval at Position 3.

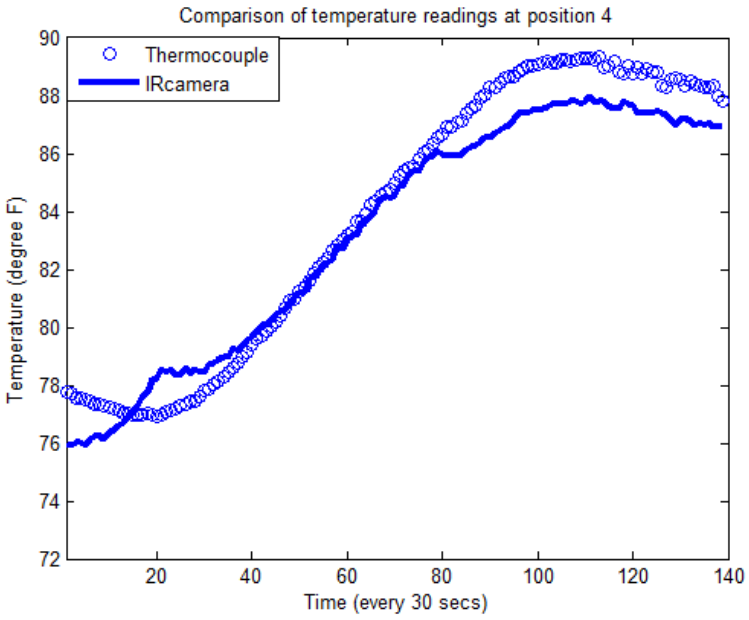

Figure 21. Comparison of infrared-camera and thermocouple measurements over a 30-second interval at Position 4.

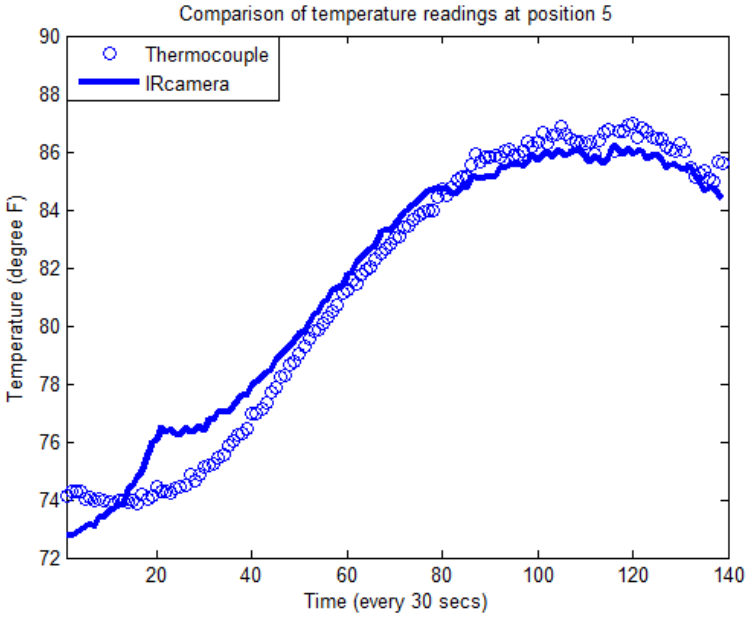

Figure 22. Comparison of infrared-camera and thermocouple measurements over a 30-second interval at Position 5.

5. SUMMARY AND FUTURE WORK

The objective of this report is to examine the use of vibro-acoustic techniques in assessing the effect of ASR on the integrity of concrete structures that are exposed to the accelerated aging conditions in a laboratory setting. A series of experiments were conducted at Vanderbilt University to provide sufficient degradation data in support of the framework for diagnosis of structure condition, and providing a prognosis, of aging concrete structures in NPPs. The main activities were:

1. Experimental setting:
    a. Three 9- × 5- × 2-in. concrete bricks were cast
    b. Various curing conditions were used to accelerate the formation of ASR gel in the three concrete bricks: (1) baseline condition – dry and normal temperature; (2) submerged in a bath of 1N NaOH solution at a temperature of 60°C; and (3) exposed to NaOH solution to increase the alkali content to 1.25%, 100% humidity (over a tube of water), and a temperature of 60°C
    c. Mechanical deformation technique using steel pegs were used to measure changes in the dimensions of the specimens
    d. NDE techniques were used for the damage detection: mechanical deformation measurements, NIRAS, VAM, and infrared thermography.
2. Data analysis results:
    a. The baseline curing condition led to the most cracking in the concrete sample (from Brick U1) followed by the brick with submerged curing (U2). During the first 5 months of curing, the brick with 100% humidity, U3, had the least structure damage (or the least nonlinearity), which indicates only a small amount of ASR gel was formed up to that point.
    b. Consistent experimental data from all three NDE techniques indicates that these techniques can be used to generate data related to an assessment of the degradation of concrete structures damaged by ASR.

Future work will focus on the following tasks during the next year:

1. Localizing and quantifying the damage and exploring embedded sensors (e.g., strain and pH)
2. Collaborating with the University of Alabama on the development of concrete specimens with distributed ASR aggregates and with localized ASR aggregates
3. Enhancing the monitoring techniques to collect high-quality data to quantify the onset of ASR and trend its progress within a concrete sample over a period of time
4. Coordinating with ongoing research activities at the University of Tennessee, Knoxville, and Oak Ridge National Laboratory to construct and monitor a large mockup and, in particular, explore the application of DIC.

Overall, this research focuses on data analysis and development of uncertainty-quantified diagnostic and prognostics models that will support continuous assessment of concrete performance. The resulting comprehensive approach will facilitate development of a quantitative, risk-informed framework that could be generalized for a variety of concrete structures and could be adapted for other passive structures. Future work will investigate how to apply the methods described in this report to realistic structures and damage scenarios.

6. REFERENCES

Agarwal, V. and S. Mahadevan, 2014, "Concrete Structural Health Monitoring in Nuclear Power Plants," *Office of Nuclear Energy Sensors and Instrumentation Newsletter*, September 2014.

ASTM C1293-08b, 2015, "Standard Test Method for Determination of Length Change of Concrete due to Alkali-Silica Reaction," ASTM International, August 2015.

ASTM C1567-13, 2013, "Standard Test Method for Determining the Potential Alkali-Silica Reactivity of Combinations of Cementitious Materials and Aggregate (Accelerated Mortar-Bar Method)," ASTM International, 2013.

Bruck, P., T. Esselman, and M. Fallin, 2012, "Digital Image Correlation for Nuclear," *Nuclear Engineering International*, April 23, 2012.

Chen, J., A. R. Jayapalan, J.-Y. Kim, K. E. Kurtis, and L. J. Jacobs, 2009, "Nonlinear wave modulation spectroscopy method for ultra-accelerated alkali-silica reaction assessment," *ACI Materials Journal*, Vol. 106, pp. 340–348.

Chen, J., A. R. Jayapalan, J.-Y. Kim, K. E. Kurtis, and L. J. Jacobs, 2010, "Rapid evaluation of alkali-silica reactivity of aggregates using a nonlinear resonance spectroscopy technique," *Cement and Concrete Research*, Vol. 40, No. 6, pp. 914–923.

Chen, X. J., J.-Y. Kim, K. E. Kurtis, J. Qu, C. W. Shen, and L. J. Jacobs, 2008, "Characterization of progressive microcracking in Portland cement mortar using nonlinear ultrasonics," *NDT&E International*, Vol. 41, pp. 112–118.

Christensen, J. A., 1990, "NPAR Approach to Controlling Aging in Nuclear Power Plants," *Proceedings of the 17th Water Reactor Safety Information Meeting*, Washington, D.C., NUREG/CP-0105, Vol. 3, pp. 509–529.

Giannini, E. R., et al., 2012, *Non-Destructive Evaluation of In-Service Concrete Structures Affected by Alkali-Silica Reaction (ASR) or Delayed Ettringite Formation (DEF)—Final Report, Part I*, FHWA/TX-13/0-6491-1, Texas A&M Transportation Institute, http://library.ctr.utexas.edu/ctr-publications/0-6491-1.pdf, October 2013.

Kim, S., D. E. Adams, H., Sohn, G. Rodriguez-Rivera, N. Myrent, R. Bond, J. Vitek, S. Carr, A. Grama, and J. J. Meyer, 2014, "Crack detection technique for operating wind turbine blades using Vibro-Acoustic Modulation," *Structural Health Monitoring*, Vol. 13, No. 6, pp. 660–670.

Kobayashi, K. and N. Banthia, 2011, "Corrosion detection in reinforced concrete using induction heating and infrared thermography," *Journal of Civil Structural Health Monitoring*, Vol. 1, No. 2, pp. 25–35.

Kreitman, K., 2011, "Nondestructive Evaluation of Reinforced Concrete Structures Affected by Alkali-Silica Reaction and Delayed Ettringite Formation," M.S. Thesis: University of Texas at Austin, Austin, Texas.

Lesnicki, K. J., J.-Y. Kim, K. E. Kurtis, and L. J. Jacobs, 2012, "Assessment of alkali-silica reaction damage through quantification of concrete nonlinearity," *Materials and Structures*, Vol. 46, pp. 497–509.

Lesnicki, K. J., J.-Y. Kim, K. E. Kurtis, and L. J. Jacobs, 2014, "Characterization of ASR Damage in Concrete Using Nonlinear Impact Resonance Acoustic Spectroscopy Technique," *NDT&E International*, Vol. 44, No. 8, pp. 721–727.

Mahadevan, S., V. Agarwal, K. Neal, D. Kosson, and D. Adams, 2014, *Interim Report on Concrete Degradation Mechanisms and Online Monitoring Techniques*, INL/EXT-14-33134, Idaho National Laboratory, September 2014.

Mahadevan, S., V. Agarwal, K. Neal, P. Nath, Y. Bao, G. Cai, P. Orme, D. Adams, and D. Kosson, 2016, *A Demonstration of Concrete Structural Health Monitoring Framework for Degradation due to Alkali-Silica Reaction*, INL/EXT-16-38602, Idaho National Laboratory, April 2016.

Naus, D., 2007, "Activities in Support of Continuing the Service of Nuclear Power Plant Safety-Related Concrete Structures," in *Infrastructure Systems for Nuclear Energy*, T. T. C. Hsu, C.-L. Wu, and J.-L. Li (eds), Chichester, United Kingdom: John Wiley & Sons, Ltd.

NextEra Energy Seabrook, 2012, "Impact of Alkali-Silica Reaction on Concrete Structures and Attachments," the Response to Confirmatory Action Letter, SBK-L-12106, from NextEra Energy Seabrook to the Nuclear Regulatory Commission (NRC), May 24, 2012.

Renshaw, J., N. Muthu, and M. Guimaraes, 2014, "Thermographic Inspection of Concrete, Tanks, and Containment Liners," *EPRI Conference*, Charlotte, North Carolina, May 8, 2014.

Ulm, F. J., O. Coussy, L. Kefei, and C. Larive, 2000, "Thermo-chemo-mechanics of ASR expansion in concrete structures," *Journal of Engineering Mechanics*, Vol. 126, No. 3, pp. 233–242.

Verhorn, K. A., 2013, "Vibro-Acoustic Modulation as a Baseline-Free Structural Health Monitoring Technique," M.S. Thesis, University of Dayton, Dayton, Ohio, https://etd.ohiolink.edu/rws_etd/document/get/dayton1374508274/inline.